nature food

Article

https://doi.org/10.1038/s43016-023-00753-6

Extreme rainfall reduces one-twelfth of China's rice yield over the last two decades

Received: 24 July 2022

Accepted: 11 April 2023

Published online: 4 May 2023

Check for updates

Jin Fu[1,13], Yiwei Jian[1,13], Xuhui Wang[1,13], Laurent Li[2], Philippe Ciais[3,4], Jakob Zscheischler[5], Yin Wang[6], Yanhong Tang[6], Christoph Müller[7], Heidi Webber[8], Bo Yang[9], Yali Wu[10], Qihui Wang[1], Xiaoqing Cui[1], Weichen Huang[1], Yongqiang Liu[11], Pengjun Zhao[12], Shilong Piao[1] & Feng Zhou[1] ✉

Extreme climate events constitute a major risk to global food production. Among these, extreme rainfall is often dismissed from historical analyses and future projections, the impacts and mechanisms of which remain poorly understood. Here we used long-term nationwide observations and multi-level rainfall manipulative experiments to explore the magnitude and mechanisms of extreme rainfall impacts on rice yield in China. We find that rice yield reductions due to extreme rainfall were comparable to those induced by extreme heat over the last two decades, reaching 7.6 ± 0.9% (one standard error) according to nationwide observations and 8.1 ± 1.1% according to the crop model incorporating the mechanisms revealed from manipulative experiments. Extreme rainfall reduces rice yield mainly by limiting nitrogen availability for tillering that lowers per-area effective panicles and by exerting physical disturbance on pollination that declines per-panicle filled grains. Considering these mechanisms, we projected ~8% additional yield reduction due to extreme rainfall under warmer climate by the end of the century. These findings demonstrate that it is critical to account for extreme rainfall in food security assessments.

Extreme climate events have been recognized as a major risk induced by climate change[1]. Agricultural ecosystems are among the most vulnerable to climate extremes, resulting in declines in crop production (through either yield or harvested area)[2]. For example, climate anomalies have been shown to account for as much as a third of the observed anomalies in global crop yields[3,4], with extreme events playing a particularly important role[5]. The consequences of such yield anomalies vary from fluctuations in food prices to destabilized food supply and famines[6]. As such, understanding the impacts of extreme climate events on crop yield is critical for adapting food systems to future climate

[1]Institute of Carbon Neutrality, Laboratory for Earth Surface Processes, College of Urban and Environmental Sciences, Peking University, Beijing, China. [2]Laboratoire de Météorologie Dynamique, CNRS, Sorbonne Université, Paris, France. [3]Laboratoire des Sciences du Climat et de l'Environnement, LSCE, Gif sur Yvette, France. [4]Climate and Atmosphere Research Center (CARE-C), The Cyprus Institute, Nicosia, Cyprus. [5]Department of Computational Hydrosystems, Helmholtz Centre for Environmental Research–UFZ, Leipzig, Germany. [6]Institute of Ecology, Laboratory for Earth Surface Processes, College of Urban and Environmental Sciences, Peking University, Beijing, China. [7]Potsdam Institute for Climate Impact Research (PIK), Member of the Leibniz Association, Potsdam, Germany. [8]Leibniz Centre for Agricultural Landscape Research, Müncheberg, Germany. [9]Key Laboratory of Nonpoint Source Pollution Control, Institute of Agricultural Resources and Regional Planning, Chinese Academy of Agricultural Sciences, Beijing, China. [10]National Engineering Laboratory for Lake Pollution Control and Ecological Restoration, Chinese Research Academy of Environmental Sciences, Beijing, China. [11]State Key Laboratory of Plant Genomics, Institute of Genetics and Developmental Biology, Chinese Academy of Sciences, Beijing, China. [12]School of Urban Planning and Design, Peking University Shenzhen Graduate School, Shenzhen, China. [13]These authors contributed equally: Jin Fu, Yiwei Jian, Xuhui Wang. ✉e-mail: zhouf@pku.edu.cn

change and thus contributing to food security for the growing global populations. Recent studies have focused on elucidating impacts of drought[7,8], extreme heat[9,10] and cold spells[11], but the impact of extreme rainfall on yields remains largely uncertain[12,13].

Estimating the yield loss due to extreme rainfall needs to assess the magnitude of extreme rainfall and timing of crop exposure, both of which are highly heterogeneous over space and time. Spatially, previous studies indicate that yield statistics and climate variables aggregated at administration zones have probably smoothed out the highly localized extreme rainfall events, which could have resulted in non-significant and weaker impact of extreme rainfall than heat and drought reported on the basis of national statistics[2,12]. Temporarily, the exposure of crops to extreme rainfall can be dismissed if using climate data with coarse temporal resolution to explore the climate–yield relationships[12]. The lack of clear mechanistic evidence for extreme rainfall impacts has also rendered crop modellers to dismiss their potential effects in projecting the impacts of climate change[14], despite the expected increase in occurrence of extreme rainfall[15].

Rice is the primary calorie source for more than 50% of the world's population, with the largest production in China[16]. This crop is generally considered to be strongly tolerant to extreme rainfall, though this may be an artefact of relatively intense irrigation and drainage management that minimizes adverse effects of rainfall anomalies. While the impacts of extreme rainfall through secondary processes (for example, waterlogging[17]) have been well documented, the impacts through biophysical or biochemical processes remain poorly investigated. In this Article, we used long-term nationwide observations and multi-level rainfall manipulative experiments to explore the magnitude and mechanisms of extreme rainfall impacts on rice yield in China. We further improved a process-based crop model by explicitly accounting for the biophysical or biochemical mechanisms to hindcast and project the yield responses to extreme rainfall across China. This combination of field observation, manipulative experiment and model simulation enables us to address three questions here: What is the magnitude and pattern of change in rice yield due to extreme rainfall over the last two decades? What are the key mechanisms determining rice yield response to extreme rainfall? How strongly do changes in extreme rainfall impact future rice yield?

Results

Evidence from nationwide observations

We used a window searching strategy to isolate changes in rice yield (ΔY) induced separately by an extreme climate event for each site and rice type from the nationwide observations in 1999–2012 (Methods and Supplementary Text 1), yielding 707 ΔY data at 114 sites (Supplementary Fig. 1b and Supplementary Data 1). While the data were by far limited and not homogeneously distributed, they represented climate heterogeneity across China's rice production areas quite well (Supplementary Text 2). These data show that extreme rainfall induced a significant yield reduction by 7.6 ± 0.9% (one standard error) in China ($n = 217$, $P < 0.001$, Fig. 1a). Counter-intuitively, the yield reduction due to extreme rainfall was comparable to that due to extreme heat (5.4 ± 1.7%, $n = 61$, $P = 0.27$), and larger than the reductions related to drought (4.2 ± 1.1%, $n = 152$, $P = 0.01$), extreme cold (3.7 ± 0.9%, $n = 163$, $P = 0.002$) and the remaining extreme events (for example, hail, typhoon and tropical cyclones, 2.9 ± 1.1%, $n = 114$, $P < 0.001$, Fig. 1a). The larger ΔY for extreme rainfall in relative to other extreme events was robust when comparing different extreme events with similar probability of occurrence (Supplementary Fig. 2), and was not strongly influenced by the methods used (window searching strategy versus superposed epoch analysis[2], time series analysis[13] and panel regression model[18]; Fig. 1a and Supplementary Fig. 3). Spatial analyses further confirm that the negative effects of extreme rainfall on rice yield are more pervasive and stronger than those of other extreme events, even though record yield reductions ($\Delta Y < -20\%$) can arise from any type of extreme event considered here (Fig. 1b–f and Supplementary Fig. 4).

To identify the potential factors determining the magnitude of extreme rainfall impacts, correlation analyses were performed between ΔY and extreme rainfall parameters. Extreme rainfall is defined as hourly precipitation exceeding the threshold that is the 99th percentile of growing-season hourly precipitation over the base period 1981–2012 for each site. An extreme rainfall event is defined as a time period that involved at least 1 h with extreme rainfall and for which the break duration between hourly precipitation does not exceed 6 h (ref. 19). On the basis of the hourly precipitation data from the China Meteorological Administration (CMA), five extreme rainfall parameters were quantified during the rice growing season (Supplementary Data 1), including intensity as the maximum hourly precipitation when exceeding the threshold (cm h^{-1}), total intensity as the sum of hourly precipitation when exceeding the threshold (cm), frequency as the fraction of hours of extreme rainfall (%), proportion as the sum of hourly precipitation that exceeds the threshold divided by the growing-season total precipitation (%) and event amount as the precipitation amount averaged for extreme rainfall events (cm per event). The correlation analyses show that extreme-rainfall-induced ΔY was negatively correlated with intensity and event amount of extreme rainfall occurred during rice growing season, rather than with the total intensity, frequency or proportion of extreme rainfall (Supplementary Fig. 5a). The combining results from the Kruskal–Wallis rank sum test and the Dunn's test affirm that the repeated extreme rainfall does not add to additional yield loss (Supplementary Fig. 5b). These relationships are robust against variations in the definitions of extreme rainfall (exceeding 95th, 99th or 99.9th percentile of growing-season hourly precipitation over the base period) and of break duration between hourly precipitation (2, 6 or 12 h) for consecutive extreme rainfall events (Supplementary Table 1), confirming the key driving indicators are extreme rainfall intensity and event amount rather than repeated frequencies.

The nationwide observations also indicated that rice might be more vulnerable to extreme rainfall than rainfed crops. Although with large site-to-site differences, we found that rice yield was negatively affected by rainfall when intensity exceedingly around 20 cm h^{-1} (Supplementary Fig. 6). This threshold seems lower than that detected in ref. 12 on rainfed maize and soybean over the US Midwest. This is understandable since yield of largely rainfed crops may benefit from extreme rainfall by improving plant available water or buffering drought[8,20], while intensively irrigated rice benefits less from the compensating effects. More soluble nutrient loss from rice fields than that of maize and soybean also contribute to the high sensitivity to extreme rainfall[21,22].

Experimental tests of rainfall–rice yield relationship

To isolate the mechanisms leading to extreme rainfall impacts on ΔY, we established a series of rainfall manipulative experiments in 2018 and 2019 at the Jingzhou Agrometeorological Experimental Station located in Central China (Fig. 2a and Supplementary Fig. 7). In the experiments, we established four rainfall levels of intensity and event amount to broadly represent extreme rainfall heterogeneity across China's rice fields. To test if the impacts differ by growth phases, rainfall manipulation was conducted for each or their combination of the three phases (that is, vegetative phase when tillers are formed, reproductive phase when spikelets reach anthesis and ripening phase when grains are filled). We quantified ΔY between treatment and control plots for which two replicates were considered, and converted the manipulative rainfall to equivalent natural rainfall in terms of measured kinetic energy (Methods). ΔY was −1.1 ± 0.3% and −0.6 ± 0.1% in response to 1 cm increase in extreme rainfall intensity and event amount, respectively. These effect sizes were also statistically the same between the two experimental years (Supplementary Fig. 8a,b). Analyses of changes in yield components indicated that ΔY were mostly caused by declines in effective panicles per unit land area (EP) and filled grains per panicle (FG), accounting for 22% to 25% and 71% to 75% of ΔY, respectively,

https://doi.org/10.1038/s43016-023-00753-6

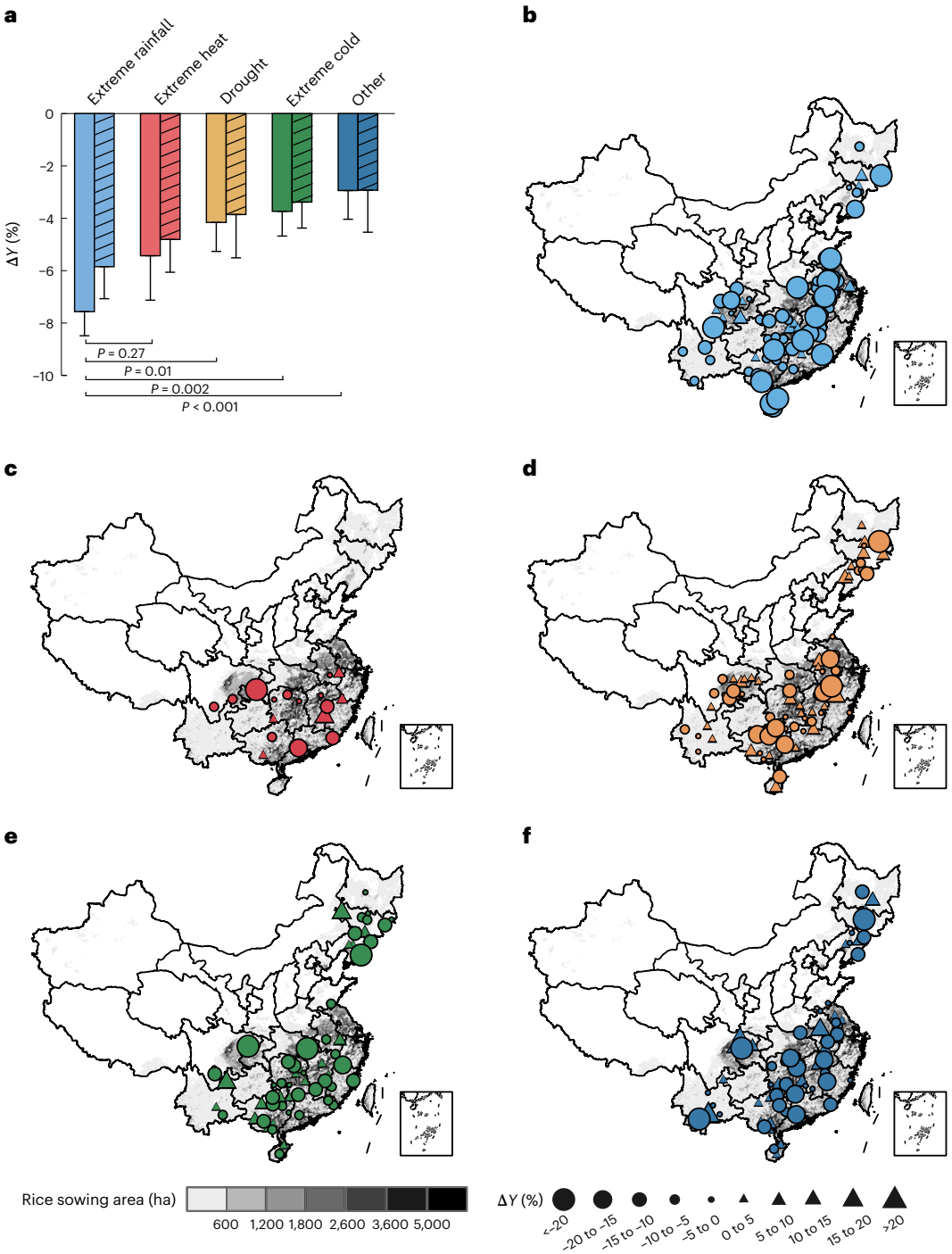

Fig. 1 | Changes in rice yield (Δ*Y*) induced by extreme climate events in China. **a**, Δ*Y* (mean ± standard error) quantified by the window searching strategy (left column of each pair) and mean of three other methods[2,13,18] (right column of each pair, $n = 3$; see Supplementary Text 1). Statistical significance of the differences in mean Δ*Y* between extreme rainfall and other events was quantified by the two-sided bootstrap *t*-test. For the left column of each pair, $n = 217$ for extreme rainfall, $n = 61$ for extreme heat, $n = 152$ for drought, $n = 163$ for extreme cold and $n = 114$ for the other events. **b**–**f**, Patterns of Δ*Y* induced by extreme rainfall at 82 sites (**b**), extreme heat at 18 sites (**c**), drought at 73 sites (**d**), extreme cold at 61 sites (**e**) and the other events at 68 sites (typhoon and tropical cyclones; **f**). Each point in **b**–**f** represents the location of a given extreme climate event with Δ*Y*, with size of the symbols showing the mean percent change over the period 1999–2012. The base map of the country boundaries was from the Global Administrative Areas dataset (https://gadm.org).

whereas decreased grain weight (GW) contributed to only approximately 1.4% to 6.0% (Fig. 2c–e and Supplementary Fig. 8c). Extreme rainfall impacts on yield components depend on growth phase: extreme rainfall in the vegetative phase mainly reduced EP, while in the reproductive phase, it mainly reduced FG. (Fig. 2c,d).

The damages of extreme rainfall result from biophysical and biochemical processes, and secondary processes such as waterlogging[17], stem laydown[23] and disease development[24,25]. In our experiments, no plants were washed away, fell or infected due to rainfall manipulation. We therefore hypothesized that the growth phase-dependent effects

https://doi.org/10.1038/s43016-023-00753-6

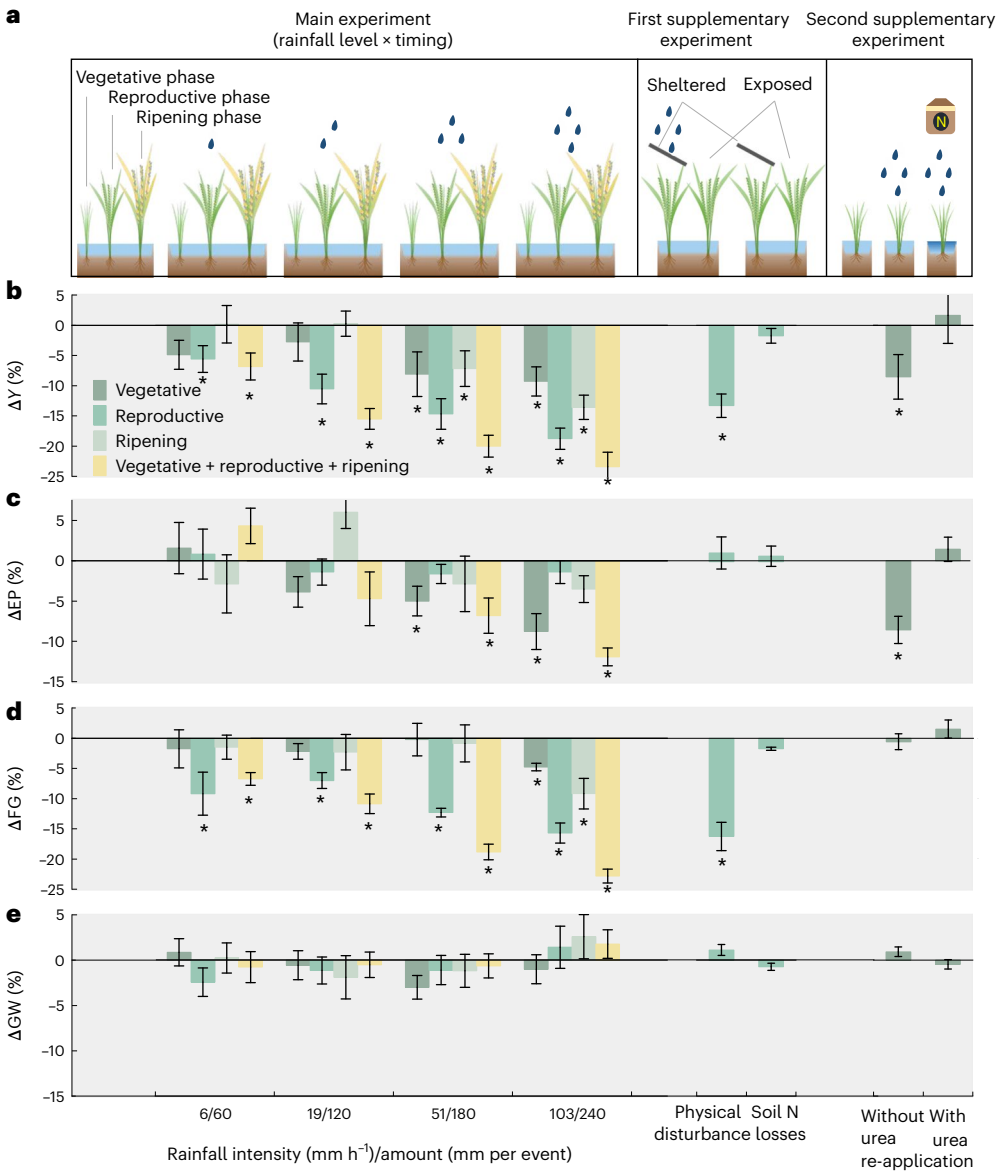

Fig. 2 | Effects of simulated rainfall on rice yield and yield components. **a**, Experimental set-up. **b**–**e**, Relative changes in rice yield (Δ*Y*; **b**), effective panicles per unit land area (ΔEP; **c**), filled grains per panicle (ΔFG; **d**) and grain weight (ΔGW; **e**). For the second supplementary experiment, the urea re-application rate (that is, 28.8 kg N ha^{-1}) is equal to the average N losses observed from the treatment plots using the same rainfall amount during vegetative phase in main experiments. Sample size is 4 for each treatment, but 3 for each supplementary experiment. Data are presented as mean ± standard error. The asterisk indicates for the significant difference with zero based on two-sided *t*-test, with $P < 0.05$.

of extreme rainfall mainly result from biophysical and biochemical mechanisms in reducing rice yield, that is, high extreme rainfall intensity reduces per-panicle filled grains through physical disturbance (in terms of kinetic energy) on pollination[26], and high extreme rainfall event amount stresses tillering through inducing soil N losses[12]. To test these hypotheses, we conducted two supplementary experiments using the maximum rainfall level (103 mm h^{-1} for natural rainfall intensity or 240 mm per event for event amount) in 2021 (Methods).

In the first supplementary experiment, we sheltered half of each rice plot during the reproductive phase so that the sheltered halves of treatment were affected by extreme rainfall only through its effects on soil N losses, but not direct physical disturbance (Fig. 2a and Supplementary Fig. 9). We found FG in the sheltered halves of treatment show little difference (<2.0%) with the control, while FG in the exposed halves of treatment decreased by 18.0 ± 2.6% (Fig. 2). The empty or shrunken grains were found mostly in the upper part of the panicles of the exposed halves of treatment (Supplementary Fig. 10), further supporting that FG were reduced by the physical disturbance that prevents successful pollination, a critical process of yield formation.

The second supplementary experiment isolates the effects of soil N losses induced by extreme rainfall event amount during the vegetative phase (Supplementary Fig. 9a). We supplied additional urea to half of the treatments, so that if there was a soil N loss induced by the extreme rainfall, it would be compensated. We found that urea re-application could help maintain N uptake per tiller, and thus successfully stabilized EP and rice yield (Fig. 2). Treatments that did not compensate for N losses caused proportionally similar declines in N uptake per tiller and thereby EP ($R^2 = 0.67$ and 0.61, respectively, $P < 0.001$; Supplementary Fig. 11). These findings confirm that the reduced EP was primarily attributable to extreme rainfall event amount that limits soil N availability and crop N uptake causing lower yields.

https://doi.org/10.1038/s43016-023-00753-6

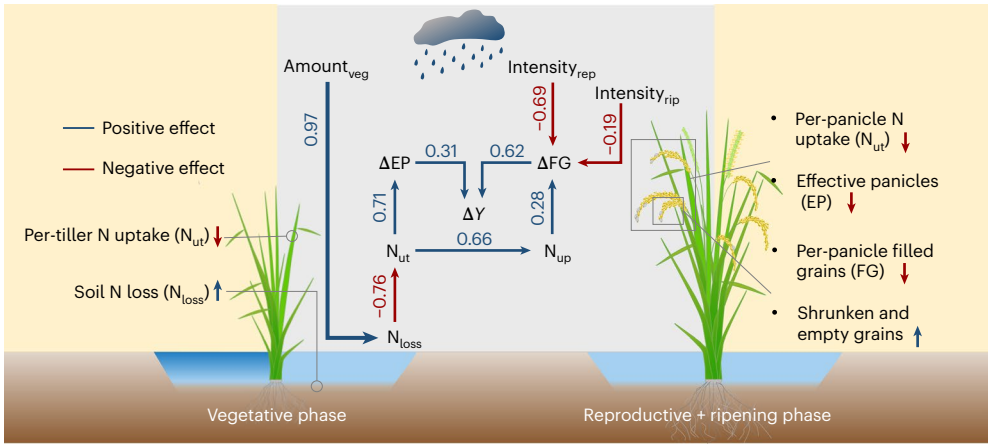

Fig. 3 | Schematic diagram of extreme rainfall impacts on rice yield. Best-explaining SEM illustrating major pathways through which extreme rainfall reduced rice yield ($\chi^2 = 22.8$, $P = 0.530$, d.f. = 24, $n = 32$). Single-headed arrows indicate the direction of causation identified by the structural equation modelling. Blue (red) arrows indicate significant positive (negative) effects ($P < 0.05$). Arrow width is proportional to the strength of the relationship, which is characterized by standardized path coefficients showing next to arrows. The coefficients can be interpreted as the change in the dependent variable when the independent variable changes by one standard deviation. Amount$_{veg}$, extreme rainfall event amount in vegetative phase; Intensity$_{rep}$ and Intensity$_{rip}$, extreme rainfall intensity in reproductive and ripening phases, respectively; ΔY, relative changes in rice yield.

Ultimately, we conducted a series of structural equation models (SEMs) to test potential pathways by which extreme rainfall reduces rice yield (Supplementary Fig. 12). The SEMs were formulated on the basis of the experimental measurements of rice yield, physiological factors and physical and chemical factors in 2018 and 2019 (Methods). The SEM including the direct pathways of rainfall-induced physical disturbance and soil N losses shows the best performance (Fig. 3), explaining 56% of the overall variance in rice yield reductions. This suggests that both pathways are primary mechanisms explaining ΔY, whereas other potential mechanisms (for example, changes in photosynthesis, leaf area index, phosphorous loss, and phosphorous and potassium absorptions) do not show significant effects (Supplementary Fig. 12b–e). In addition to these two direct pathways, the best-explaining SEM also identified an indirect pathway, that is, rainfall-induced N losses during the vegetative phase, which may also limit per-panicle N uptake during the reproductive phase thereby decreasing FG (Fig. 3).

Crop model improvements for assessing ΔY

Correctly representing the mechanisms through which extreme rainfall reduces rice yield is critical for diagnosing and projecting spatiotemporal variations in rice yield. We introduced the physical disturbance module of extreme rainfall on rice yield in ORganizing Carbon and Hydrology in Dynamic EcosystEms for crops (ORCHIDEE-crop)[27], which is a process-based crop model including the representation of single, early and late rice types, paddy rice irrigation and a detailed soil hydrology model[28]. The direct and indirect pathways of extreme rainfall through soil N losses was also introduced into the model (Methods and Supplementary Table 2). The model with the extreme rainfall processes was calibrated by the experimental observations in 2018–2019, and then validated by the nationwide observations in 1999–2012. The results show that the model, in contrast to that without the extreme rainfall processes, can reproduce the rice yield variability due to year-to-year weather variations and extreme rainfall treatments (the coefficient of determination (R^2) of 0.88 in 2018 and 0.78 in 2019, Supplementary Figs 13a,b), and robustly capture the spatiotemporal heterogeneity of ΔY induced by extreme rainfall ($R^2 = 0.41$, Supplementary Fig. 13c).

We then used the high-resolution global precipitation measurement (GPM) datasets[29] to drive the model with the extreme rainfall processes over China in 2001–2016 (Methods). On average, the model with the extreme rainfall processes hindcasts lower rice yields due to the extreme rainfall by 8.1 ± 1.1% (weighted by sowing area, one standard error for interannual variability) for all rice types, 8.3 ± 1.0% for single rice, 8.6 ± 1.0% for early rice and 7.6 ± 1.3% for late rice (Supplementary Figs 14a–c). Higher ΔY were simulated eastern China and southern coastal regions that experienced higher rainfall intensities (Supplementary Figs 14a–c). Factorial model simulations show that physical disturbance induced by extreme rainfall was the most important determinant across 47–95% of rice sowing areas (Supplementary Figs 14d–f), leading to yield losses of 3.9% for single rice, 5.1% for early rice and 4.1% for late rice. Extreme rainfall-induced N losses dominated the ΔY mainly in Anhui and Jiangsu provinces where both N application rates[30] and extreme rainfall event amount were relatively high[31] (Supplementary Figs 14g–i).

Projected impacts of future change in extreme rainfall

Since extreme rainfall was found to have significant impacts on historical rice yields, a process that was neglected in previous process-based crop model projections under climate change[32,33], we made a attempt to project the risk of future rice yield to changing extreme rainfall dynamics. We used the high-resolution climate projection by the Institute Pierre-Simon Laplace (IPSL) model zoomed over China[34], which performed well in reproducing the spectral properties of rainfall including extreme events[35], to drive the model with the extreme rainfall processes under two climate scenarios (Representative Concentration Pathways (RCPs) 4.5 and 8.5; Methods). Considering extreme rainfall impacts led to greater projected yield reductions by the end of this century (2085–2100; Fig. 4). On average, extreme rainfall induces an additional yield reduction of 7.6% (weighted by sowing area) in China on top of other climate-change-induced impacts under RCP 4.5. We then ranked the additional yield reductions in grid cells from the largest to smallest and calculated the cumulative sowing area affected by a given additional yield change, and found that the sowing areas with additional yield reduction of >7.6% accounted for 58% for early rice, 39% for single rice and 29% for late rice (Fig. 4a). Rice is projected to suffer from extreme rainfall events the most over northeast China and southeast coastal regions (Fig. 4b–d). However, additional yield reductions were projected to be weaker under RCP 8.5 relative to RCP 4.5 (Fig. 4e–h), with the national mean reduction due to extreme rainfall of 5.4%, mainly because of larger rice yield reduction induced by stronger warming and carbon dioxide concentrations under RCP 8.5

https://doi.org/10.1038/s43016-023-00753-6

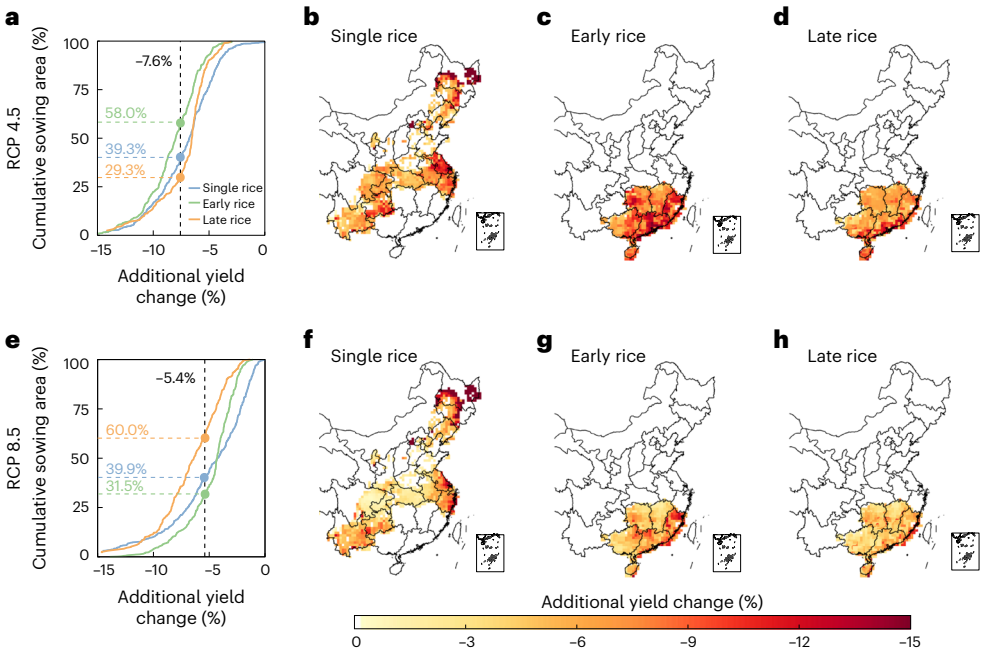

Fig. 4 | Future projections of additional yield change induced by extreme rainfall. a,**e**, Cumulative proportions of sowing area affected by a given additional yield change under RCP 4.5 (**a**) and RCP 8.5 (**e**). Black dashed lines represent the national means (−7.6% and −5.4%), and the numbers represent the cumulative proportions of sowing area affected by exceeding the national means. **b**–**d**, Patterns of Δ*Y* under RCP 4.5 for single rice (**b**), early rice (**c**) and late rice (**d**). **f**–**h**, Same as **b**–**d** but under RCP 8.5. The base map of the country boundaries was from the Global Administrative Areas dataset (https://gadm.org).

together with no differences in projected extreme rainfall between the two scenarios (Supplementary Fig. 15). These projections highlight the increasing risk of rice yield reductions induced by extreme rainfall. There is an urgent need to consider this risk in planning climate change adaptations, such as guaranteeing N availability to maintain tillering effectiveness[36], avoiding excessive losses to the environment[30] and breeding for rainfall-tolerant rice varieties[37].

Discussion

While both nationwide observations and model simulations indicated approximately 8% of rice yield lost in China due to extreme rainfall, we note that our analyses are subject to several sources of uncertainties. On the observation side, due to rigorous screening criteria to isolate extreme rainfall impacts from other extreme events, rice yield assessment has been eliminated over the Southeast Coast where extreme rainfall is strong (Supplementary Figs. 1b and 16), probably underestimating the extent of extreme rainfall induced Δ*Y*. On the modelling side, extreme rainfall intensity and event amount used for driving the historical simulations across China were from the half-hourly and 0.1° GPM dataset, which is well represented for but still did not fully capture the observed heaviest rainfall extremes during rice growing seasons (Supplementary Fig. 17). Thus, our estimates of extreme rainfall impact on rice yield should be viewed as a conservative assessment. Another source of uncertainty is related to the set-up of our manipulative experiments. The experiments were conducted on cloudy days to mimic natural rainfall conditions, but muted the effects of secondary processes. These secondary processes may cause rice diseases and lodging that can further compound rice yield responses[13,24]. Moreover, our experiment focused on uncovering mechanisms of extreme rainfall impacts under regular management, without climatic adaptations, which introduces additional uncertainties in future projection.

Although we focused on rice yields in China, which is the largest rice producer globally, attention to other rice-producing regions may yield critical insights into the biogeography and generalizability of our findings. Compared with China, rice fields in South and Southeast Asia have smaller N application rates and larger fractions of rainfed rice (Supplementary Fig. 18). Extreme rainfall in these regions may lead to a lower risk of soil N losses and thus lower impacts on tillering. However, these regions were more exposed to extreme rainfall given much higher extreme rainfall intensity (Supplementary Fig. 16b), and thus subject to higher risk of physical disturbance. Since extreme rainfall impacts results from direct physical disturbance on pollination across 70% of China's rice fields (Supplementary Figs 14j-l), rice yield reductions in South and Southeast Asia should also be notable. Previous projections of rice yield response to climate change without considering the extreme rainfall impacts (for example, Webber et al.[14], Rosenzweig et al.[32], Jägermeyr et al.[33] and Iizumi et al.[38]) have probably been overly optimistic in this regard.

The impacts of extreme rainfall on other staple crops such as wheat and maize remain to be explored. Although the magnitude and mechanistic representation of rice yield response to extreme rainfall may not be directly applicable to other crops, our research paradigm that combines field observations, manipulative experiments and processed-based modelling is well transferable. Unlike rice, a sizable fraction of upland crops were rainfed or under different irrigation-drainage systems[39]. Thus extreme rainfall effect may not be stronger than droughts, and the sensitivity of tillering and pollination processes in response to extreme rainfall may also be different from what we observed here. Therefore, a major research challenge remains to assess the global extreme rainfall impacts for all cereal crops.

Methods

Analysis of nationwide observational data

Yield change induced by extreme climate events. We collected field observations of rice yield and extreme climate events from the national agrometeorological observation network that is run by the CMA. This network covers the rice fields for single rice in Northeast and Central China and early and late rice in South China. All sites in the network refer to irrigated rice systems, which account for 99% of rice fields in China (Supplementary Fig. 18). The network observed extreme climate

events occurring in the rice growing seasons over the period 1999–2012 at 356 sites, but only 166 of them provide information for rice yields over the same period. In total, it provides rice yield of 2,304 observations and extreme climate events of 8,595 observations. Rice yield is defined as actual production divided by the hectare of harvested area. Extreme climate events are recorded on given days for each site and are sorted into five broad categories, that is, extreme heat, extreme cold, extreme rainfall, drought and the other events (see definitions in Supplementary Table 3).

We used a window searching strategy to quantify the change in rice yield (ΔY) induced by each extreme climate event. ΔY is defined as the relative difference in yield between the treatment and control cases (in %) from the same site and rice type, where in the treatment rice has been exposed to a given extreme event, and in the control rice has not been exposed to that event and other extreme events either did not occur or were the same as in the treatment. As such, control and treatment pairs are from the same site with the same rice type but different years. We adopted a 7-year moving window[2] to identify all available control–treatment pairs from the nationwide observations, yielding 707 pairs from 114 sites for quantifying the difference between control and treatment (Supplementary Fig. 1b and Supplementary Data 1). However, the difference for each pair can also be attributed to changes in rice cultivar, phenology and the interannual variations in climate condition. As such, we detrended rice yield to exclude the effects from changes in rice cultivar and phenology, and then used a panel regression model to exclude the effects from interannual weather variability. Subsequently, we isolated ΔY related to each extreme climate event for each site and rice type as follows:

$$\Delta Y_{i,t,u,m} = \frac{\left(YT^{de}_{i,t,u,m} - YT^{fit}_{i,t,u,m}\right) - \left(\overline{YC}^{de}_{i,k,u,m} - \overline{YC}^{fit}_{i,k,u,m}\right)}{\overline{YC}^{de}_{i,k,u,m}} \times 100\%, \quad (1)$$

where t, k, i, u and m refer to year of the treatment, year of the control, site, rice type and event type, respectively. $YT^{de}_{i,t,u,m}$ refers to the detrended yield in the treatment. $YT^{fit}_{i,t,u,m}$ refers to fitted yield after excluding effect of interannual climate variation in the treatment. $\overline{YC}^{de}_{i,k,u,m}$ and $\overline{YC}^{fit}_{i,k,u,m}$ refer to the mean rice yield in the control after being detrended and fitted, respectively, if identifying multiple controls. The detailed methods are provided in Supplementary Text 1 with examples in Supplementary Fig. 19.

The t-test was applied to estimate the significance of the difference in ΔY between extreme rainfall and other extreme events. To ensure that the unequal sample size of different extreme events did not affect the significance estimates, we ran a bootstrap t-test with 1,000 replicates using the R package MKinfer v.0.5. In addition, we calculated the percentiles of the extreme events occurred in year of the treatment relative to the base period 1981–2012, and found that most of them exceed 95th percentile (Supplementary Fig. 2a–d). However, these percentiles are not completely consistent among the events. To test the robustness of the differences in ΔY, we compared the effects of different extreme events with similar percentiles, that is, 95th to 99th (or 99th to 99.8th) percentiles for extreme heat and rainfall and 1st to 5th (or 0.2nd to 1st) percentiles for extreme cold and drought (Supplementary Fig. 2e,f).

Correlation between ΔY and extreme rainfall parameters. We conducted correlation analyses of the extreme rainfall induced ΔY against five parameters to identify the potential factors determining the magnitude of extreme rainfall impacts. Besides, the Kruskal–Wallis rank sum test and the Dunn's test were applied to test if ΔY is sensitive to the repeated extreme rainfall (1, 2, 3 and ≥4 times). We also tested if ΔY in response to extreme rainfall is dependent on the definitions of extreme rainfall based on different thresholds (95th, 99th or 99.9th percentile) and of extreme rainfall event based on break duration (≤2, 6 or 12 h) (Supplementary Table 1).

Rainfall manipulative experiments

Plants and cultivation condition. The experimental site is at the Jingzhou Agrometeorological Experimental Station in Hubei Province, China (30° 21′ N, 112° 09′ E; Supplementary Fig. 7a). It is characterized as subtropical humid monsoon climate, with a mean air temperature of 16 °C and a mean precipitation of 1,095 mm per year. Soil is classified as Hydragric Anthrosol (Supplementary Table 4). Rice seedling nurseries were managed under the water regime of continuous flooding. Seedlings of rice (*Oryza sativa* L.) were transplanted at 30 day seedling ages with a hill spacing of 0.33 × 0.33 m (9 hills m^{-2}), and harvested after 103 days. Rice fields were managed using yield-oriented optimal fertilizer applications. Further details on cultivation condition can be found in Supplementary Fig. 7b.

Main experiment. The rainfall manipulative experiment was conducted from 2018 to 2019, spanning two rice growing seasons. The experiment consisted of ambient control and factorial treatments with two replicates, and was designed for extreme rainfall level–timing combinations (Supplementary Fig. 7c), with the results in Supplementary Data 1. The treatments comprised four levels of extreme rainfall intensity and event amount in each or all of the three growth phases (that is, vegetative, reproductive and ripening phases), as they impact crop yield through different mechanisms, for instance, extreme rainfall with high-intensity damage plant tissue[40], whereas that with large event amount limits crop uptake through increasing soluble nutrient losses and waterlogging[12,17]. There was a total of 34 plots, each of which had an area of 6 m^2 (2 m × 3 m) and was completely isolated by plastic-covering levees and impervious plates at a 0.5 m distance in between. Throughout the experiment, all plots were subjected to the same agricultural management practices. To avoid the border effects, we use independent-samples t-test to compare the yield of ambient control with that of three plots nearby, with each plot owing 150 m^2 (25 m × 6 m) with the same agricultural management practices, and found no significant differences during three rice growing seasons ($P > 0.05$, Supplementary Fig. 20a).

We manipulated rainfall levels by running the artificial rainfall manipulation system (NLJY-10, Nanlin Electronics) for 1 h on two replicates for each treatment, with the rainfall amount of 60, 120, 180 and 240 mm. For more consistent estimates on the extreme rainfall impacts in both the field and the experiment, we thus measured the kinetic energy of manipulative rainfalls using the laser precipitation disdrometer (OTT Parsivel[2], Hach), which is equivalent to the natural rainfall intensities of 6, 19, 51 and 103 mm h^{-1} (refs. 41,42). These rainfall levels represent most of the broad range of growing-season rainfall extremes (exceeding the 99th percentile) across China's rice fields (that is, 8–143 mm h^{-1} and 12–526 mm per event observed during 1999–2012). To approximate the natural rainfall condition, rainfall manipulation was conducted in cloudy daytime for vegetative and ripening phases, but for reproductive phase specifically at 8:00–13:00 when spikelets reach anthesis in experimental site. To minimize the impact of waterlogging, ponded water was discharged within 12 h after rainfall manipulation if the depth exceeds 100 mm.

For each plot, we measured leaf area index, total tiller number and dry weights of leaf, stem and panicle, which were determined from three hills with an average number of tillers (Supplementary Data 1). All leaves, stems and panicles were oven dried (DHG500, SUPO Co.) at 75 °C for at least 72 h, before analysing N, P and K contents using a continuous flow analyser (Elementar). We measured net photosynthesis of three flag leaves at two photosynthetic photon flux densities of 1,500 and 600 μmol m^{-2} s^{-1} using Li6400 (Li-Cor Inc.). These measurements were conducted at seedling, at maturity and during three growth phases. Net photosynthesis was measured before and after each rainfall manipulation. In addition, for each treatment, we observed N and P losses via runoff and leaching during the period from the beginning of rainfall manipulation to the time when ponded water level decreased the same as that before manipulation.

At maturity, three hills with an average number of panicles were collected from each plot to determine the yield estimated as the product of EP, FG, and GW (Supplementary Data 1). The filled grains were oven dried at 75 °C for at least 72 h, but their weights were adjusted to a fresh weight with a moisture content of 0.15 g H_2O g^{-1} (ref. 43). To determine actual yields, the filled grains from the other rice plant hills for all plots were machine threshed (OUGEDA Co.) and sun dried to reach a moisture content of 0.15 g H_2O g^{-1}. The yields for all plots were highly consistent with actual ones (Supplementary Fig. 20b,c).

We calculated relative changes in rice yield and in yield components between the controls and treatments (ΔY, ΔEP, ΔFG and ΔGW in %) to simplify comparisons among treatments. Note that the compensation relationship between ΔEP and ΔFG can be avoided in our experimental plots as rice planting distance is 30 cm (ref. 44). ΔY is equal to the sum of ΔEP, ΔFG and ΔGW, that is, $\Delta Y = \Delta EP + \Delta FG + \Delta GW$ according to the Kaya identity principle[45]. The attribution results help identify the key yield components that were most affected by extreme rainfall. We further identified in which growth phase extreme rainfall regulates the changes in key yield components.

First supplementary experiment. To isolate the mechanism driving the causal relationship between extreme rainfall and ΔFG, we ran the first supplementary experiment during the reproductive phase in July 2021. In the experiment, extreme rainfall intensity is 103 mm h^{-1} (Supplementary Fig. 9 and Data 1). For each treatment, transparent impervious film was placed above half of the plot, such that half of the plants were fully exposed to artificial rainfall and the other part was sheltered but experienced the same increases in ponded water levels and nutrient losses as the exposed part. To avoid an unintentional influence of film on rice growth, the film was also placed above a half control plots and all films were removed when the experiment ended.

FG and actual yield in exposed and sheltered parts for each plot were observed. On the basis of the observations, we attributed the effect of extreme rainfall on ΔFG into physical disturbance and soil N loss as below:

$$\text{Total}: \Delta Y = Y_{ROC} - Y_{COC}, \Delta FG = FG_{ROC} - FG_{COC}, \quad (2a)$$

$$\text{Soil N loss } (o): \Delta Y_o = Y_{RC} - Y_{CC}, \Delta FG_o = FG_{ROC} - FG_{COC}, \quad (2b)$$

$$\text{Physical disturbance } (p): \Delta Y_p = \Delta Y - \Delta Y_o, \Delta FG_p = \Delta FG - \Delta FG_o, \quad (2c)$$

where ROC and COC refer to the exposed parts for treatment and control, respectively. RC and CC refer to the sheltered parts for treatment and control, respectively. In addition, we measured the number of empty and shrunken grains at maturity as well as their distribution along panicle. Such observations elucidate how extreme rainfall influences rice pollination during reproductive phase.

Second supplementary experiment. To confirm the causal effect of extreme rainfall on ΔEP, we ran the second supplementary experiment during vegetative phase in June 2021. The experiment consisted of ambient control and two treatments with rainfall amount of 240 mm (Supplementary Fig. 9a and Supplementary Data 1). For treatments, rice plants were fully exposed to artificial rainfall on six plots, half of which were re-applied by 28.8 kg N ha^{-1} (37% of tillering fertilizer application) in the form of urea after rainfall manipulation. The re-application rate was determined as the average of observed N losses from the treatment plots using the same rainfall amount during vegetative phase in 2018 and 2019.

For each plot, we observed EP and the actual yield at maturity as well as N uptake per tiller from transplantation to panicle initiation, and tested their differences between treatments and controls using the Wilcoxon rank sum test. If no significant differences between N re-applied treatment and control but significant differences between normal treatment and control were found, the decrease in EP was attributed to N losses induced by extreme rainfall during the vegetative phase.

Path analysis. Structural equation modelling implemented in the R package 'lavaan 0.6–7' allows us to test different pathways by which extreme rainfall affects rice yield. On the basis of potential causal relationships revealed by our experiments and previous literature[12,26,46], SEMs were formulated on the basis of the experimental measurements of rice yield parameters (that is, actual yield, EP, FG, and GW), physiological factors (that is, leaf area index, total tiller number, aboveground dry weights, N, P and K uptakes and net photosynthesis) and physical and chemical factors (kinetic energy of rainfall, N and P losses via runoff and leaching) in 2018 and 2019. The insignificant paths ($P > 0.05$) were eliminated gradually until all links significantly contributed to the final model. To compare model performance, we conducted a chi-squared difference test and calculated model fit statistics (root mean square error of approximation, comparative fit index, goodness-of-fit index and adjusted R squared (R^2_{adj})). Standardized path coefficients were computed according to ref. 47, which can be interpreted as the change in the dependent variable when the independent variable changes by one standard deviation.

Process-based modelling for regional assessments

We improved the process-based crop model ORCHIDEE-crop[27,28,48] to account for direct and indirect pathways of extreme rainfall revealed by the best-explaining SEM. We then used the model with the extreme rainfall processes to hindcast and project the impacts of extreme rainfall on rice yield across China during 2001–2016 and 2085–2100 under two RCPs, 4.5 and 8.5.

Model improvement. ORCHIDEE-crop simulates crop phenology, leaf area dynamics, growth of reproductive organs, and carbon allocation and management, as well as carbon, water and energy fluxes of agroecosystems. This model has been applied globally and regionally, and found to robustly reproduce yield variability[49]. ORCHIDE-crop is suitable for this study since it has been optimized for simulating the phenology and yield of single, early and late rice types in China[27,48]. It has paddy irrigation and soil hydrology schemes[28], able to represent the typical irrigation and drainage systems for China's rice fields. It runs in a half-hourly timestep and at 0.5° grid cell, suitable for extreme rainfall of short duration, which is a challenging issue for the models running at daily timestep.

In ORCHIDEE-crop, the rice growth starts from transplanting, and the growth cycle includes three stages divided by the onset of grain filling and the physiological maturity[48]. Starting from grain filling, the quantity of dry matters accumulated in grains is calculated by applying a progressive 'harvest index' to the biomass of the plant. The daily rate of grain increment is proportional to the daily accumulated thermal unit, which could be reduced by frost and extreme heat[50]. The impacts of extreme rainfall are formulated as a factor (α) to reduce the rate of grain increment:

$$\alpha = (1 + \Delta EP + \Delta FG), \quad (3a)$$

$$\Delta EP = 0.262 \times \Delta N_{ut} - 1.644, \quad (3b)$$

$$\Delta FG = -0.00424 \times KE_{re} - 0.00115 \times KE_{ri} + 0.139 \times \Delta N_{up} - 3.676. \quad (3c)$$

These model equations were derived from the best-explaining SEM, where ΔN_{ut} and ΔN_{up} denote relative change in N uptake per tiller and N uptake per panicle during vegetative phase (%) as a function of soil N losses, respectively. KE_{re} denotes kinetic energy (J m^{-2} h^{-1}) of the maximum hourly precipitation (exceeding the 99th percentile) occurred

at 08:00–16:00 in flowering period when spikelets reach anthesis and if hourly air temperature ranges from 23 °C to 35 °C (refs. 51,52). KE_{ri} denotes kinetic energy of the maximum hourly precipitation (exceeding the 99th percentile) during ripening phase. Note that equation (3) summing ΔEP and ΔFG is suitable to diagnose and project extreme rainfall induced ΔY across China, since the rice planting distances of 17–25 cm in China are enough to avoid the compensation relationship between EP and FG[44] (Supplementary Data 1). Further details on model equations can be found in Supplementary Table 2.

Historical simulation. Two sets of historical simulations were performed for three rice types over China: (1) the comprehensive simulation (S0) that accounts both impacts of rainfall-induced physical disturbance and soil N losses on rice yield and (2) the partial simulation (S1) that only accounts the impact of physical disturbance. By comparing S0 and S1, we isolate the impact of soil N losses. The difference between yield simulations from simulation with and without the extreme rainfall processes can be attributed to the historical extreme rainfall (Supplementary Data 2); thus, we derived ΔY as below:

$$\Delta Y = \frac{\text{Yield simulation}_{\text{with}} - \text{Yield simulation}_{\text{without}}}{\text{Yield simulation}_{\text{without}}} \times 100\%. \quad (4)$$

Details on historical input data can be found in Supplementary Table 5. Specifically, we used field observed rice phenology from the CMA to interpolate 0.1° transplanting date[48]. We used the satellite-based gridded precipitation datasets (GPM IMERGv6) to quantify extreme rainfall intensities and event amounts, since it is well represented at the site scale (Supplementary Fig. 17).

Future projections. To evaluate the implications of our findings for future rice yield projections over China, we applied the ORCHIDEE-crop model with the extreme rainfall processes to simulate yield changes of three rice types under RCP 4.5 and 8.5 with present-day agricultural management practices (Supplementary Data 2). To analyse the effect of future extreme rainfall on rice yield, we estimated additional rice yield loss as the difference between yield simulations with and without the extreme rainfall processes in 2085–2100 divided by the yield simulation without the extreme rainfall processes in 2001–2016. To remove systematic deviations of the simulated historical climate, we applied the trend-preserving bias correction[53] to the IPSL projected climate change[34]. The bias correction was then applied to the climate forcing data and extreme rainfall indices during 2085–2100. Further details on input data source for future projections can be found in Supplementary Table 5.

Reporting summary

Further information on research design is available in the Nature Portfolio Reporting Summary linked to this article.

Data availability

The data from the national agrometeorological observation network and the rainfall manipulative experiments are available in Supplementary Data 1. The climate data, records of extreme climate events, rice yield and phenology at the site scale from the CMA are available at https://data.cma.cn/en. Model input data for historical simulations and future projections are available from public data depositories listed in Supplementary Table 5. The GPM IMERGv6 are available at https://disc.gsfc.nasa.gov/datasets/GPM_3IMERGHH_06/summary. Model output data for historical simulations and future projections are available in Supplementary Data 2. Source data are provided with this paper.

Code availability

Source codes for data analyses are available from https://doi.org/10.6084/m9.figshare.19801765. Source codes for process-based model are available from http://forge.ipsl.jussieu.fr/orchidee, under the French Free Software license, compatible with the GNU GPL (http://cecill.info/licences.en.html).

References

1. Field, C. B. et al. *Managing the Risks of Extreme Events and Disasters to Advance Climate Change Adaptation. A Special Report of Working Groups I and II of the Intergovernmental Panel on Climate Change* (Cambridge Univ. Press, 2012).
2. Lesk, C., Rowhani, P. & Ramankutty, N. Influence of extreme weather disasters on global crop production. *Nature* **529**, 84–87 (2016).
3. Ray, D. K., Gerber, J. S., MacDonald, G. K. & West, P. C. Climate variation explains a third of global crop yield variability. *Nat. Commun.* **6**, 5989 (2015).
4. Proctor, J., Rigden, A., Chan, D. & Huybers, P. More accurate specification of water supply shows its importance for global crop production. *Nat. Food* **3**, 753–763 (2022).
5. Vogel, E. et al. The effects of climate extremes on global agricultural yields. *Environ. Res. Lett.* **14**, 054010 (2019).
6. Hasegawa, T. et al. Extreme climate events increase risk of global food insecurity and adaptation needs. *Nat. Food* **2**, 587–595 (2021).
7. Lobell, D. B. et al. Greater sensitivity to drought accompanies maize yield increase in the US Midwest. *Science* **344**, 516–519 (2014).
8. Lesk, C. et al. Stronger temperature–moisture couplings exacerbate the impact of climate warming on global crop yields. *Nat. Food* **2**, 683–691 (2021).
9. Wang, X. H. et al. Emergent constraint on crop yield response to warmer temperature from field experiments. *Nat. Sustain.* **3**, 908–916 (2020).
10. Lobell, D. B., Sibley, A. & Ortiz-Monasterio, J. I. Extreme heat effects on wheat senescence in India. *Nat. Clim. Change* **2**, 186–189 (2012).
11. Zhang, J. Y., Li, X. M., Lin, H. X. & Chong, K. Crop improvement through temperature resilience. *Annu. Rev. Plant Biol.* **70**, 753–780 (2019).
12. Lesk, C., Coffel, E. & Horton, R. Net benefits to US soy and maize yields from intensifying hourly rainfall. *Nat. Clim. Change* **10**, 819–822 (2020).
13. Li, Y., Guan, K. Y., Schnitkey, G. D., DeLucia, E. & Peng, B. Excessive rainfall leads to maize yield loss of a comparable magnitude to extreme drought in the United States. *Glob. Change Biol.* **25**, 2325–2337 (2019).
14. Webber, H. et al. Diverging importance of drought stress for maize and winter wheat in Europe. *Nat. Commun.* **9**, 4249 (2018).
15. Seneviratne, S. I. et al. in *Climate Change 2021: The Physical Science Basis* (eds Masson-Delmotte, V. et al.) 1513–1766 (Cambridge Univ. Press, 2021).
16. Crops and livestock products. *FAOSTAT* http://www.fao.org/faostat/en/#home (2019).
17. Shaw, R. E. & Meyer, W. S. Improved empirical representation of plant responses to waterlogging for simulating crop yield. *Agron. J.* **107**, 1711–1723 (2015).
18. Zhu, P. et al. The critical benefits of snowpack insulation and snowmelt for winter wheat productivity. *Nat. Clim. Change* **12**, 485–490 (2022).
19. Wu, X. S. et al. On the event-based extreme precipitation across China: time distribution patterns, trends, and return levels. *J. Hydrol.* **562**, 305–317 (2018).
20. Lesk, C. et al. Compound heat and moisture extreme impacts on global crop yields under climate change. *Nat. Rev. Earth Environ.* **3**, 872–889 (2022).

21. Hou, X. K. et al. Detection and attribution of nitrogen runoff trend in China's croplands. *Environ. Pollut.* **234**, 270–278 (2018).
22. Gao, S. S. et al. Quantifying nitrogen leaching response to fertilizer additions in China's cropland. *Environ. Pollut.* **211**, 241–251 (2016).
23. Steiner, J. L., Briske, D. D., Brown, D. P. & Rottler, C. M. Vulnerability of Southern Plains agriculture to climate change. *Clim. Change* **146**, 201–218 (2018).
24. Mäkinen, H. et al. Sensitivity of European wheat to extreme weather. *Field Crop Res.* **222**, 209–217 (2018).
25. Reichstein, M. et al. Climate extremes and the carbon cycle. *Nature* **500**, 287–295 (2013).
26. Win, A., Tanaka, T. S. T. & Matsui, T. Panicle inclination influences pollination stability of rice (*Oryza sativa* L.). *Plant Prod Sci* **23**, 60–68 (2020).
27. Wang, X. H. *Impacts of Environmental Change on Rice Ecosystems in China: Development, Optimization and Application of ORCHIDEE-CROP Model*. PhD thesis, Peking Univ. (2016).
28. Yin, Z. et al. Improvement of the irrigation scheme in the ORCHIDEE land surface model and impacts of irrigation on regional water budgets over China. *J. Adv. Model Earth Syst.* **12**, e2019MS001770 (2020).
29. Huffman, G. J., Stocker, E. F., Bolvin, D. T., Nelkin, E. J. & Tan, J. GPM IMERG Final Precipitation L3 Half Hourly 0.1 degree x 0.1 degree V06, Greenbelt, MD. *Goddard Earth Sciences Data and Information Services Center* https://disc.gsfc.nasa.gov/datasets/GPM_3IMERGHH_06/summary (2019).
30. Cui, X. Q. et al. Global mapping of crop-specific emission factors highlights hotspots of nitrous oxide mitigation. *Nat. Food* **2**, 886–893 (2021).
31. Jian, Y. W., Fu, J., Li, B. G. & Zhou, F. Increased extreme hourly precipitation over China's rice paddies from 1961 to 2012. *Sci. Rep.* **10**, 10609 (2020).
32. Rosenzweig, C. et al. Assessing agricultural risks of climate change in the 21st century in a global gridded crop model intercomparison. *Proc. Natl Acad. Sci. USA* **111**, 3268–3273 (2014).
33. Jägermeyr, J. et al. Climate impacts on global agriculture emerge earlier in new generation of climate and crop models. *Nat. Food* **2**, 873–885 (2021).
34. Yang, H., Jiang, Z. H. & Li, L. Biases and improvements in three dynamical downscaling climate simulations over China. *Clim. Dyn.* **47**, 3235–3251 (2016).
35. Chen, W. L., Jiang, Z. H., Li, L. & Yiou, P. Simulation of regional climate change under the IPCC A2 scenario in southeast China. *Clim. Dyn.* **36**, 491–507 (2011).
36. Barbier, F. F., Dun, E. A., Kerr, S. C., Chabikwa, T. G. & Beveridge, C. A. An update on the signals controlling shoot branching. *Trends Plant Sci.* **24**, 220–236 (2019).
37. Bailey-Serres, J., Parker, J. E., Ainsworth, E. A., Oldroyd, G. E. D. & Schroeder, J. I. Genetic strategies for improving crop yields. *Nature* **575**, 109–118 (2019).
38. Iizumi, T. et al. Prediction of seasonal climate-induced variations in global food production. *Nat. Clim. Change* **3**, 904–908 (2013).
39. Meier, J., Zabel, F. & Mauser, W. A global approach to estimate irrigated areas—a comparison between different data and statistics. *Hydrol. Earth Syst. Sci.* **22**, 1119–1133 (2018).
40. Lepore, C., Allen, J. T. & Tippett, M. K. Relationships between hourly rainfall intensity and atmospheric variables over the contiguous United States. *J. Clim.* **29**, 3181–3197 (2016).
41. Atlas, D., Srivastava, R. C. & Sekhon, R. S. Doppler radar characteristics of precipitation at vertical incidence. *Rev. Geophys.* **11**, 1–35 (1973).
42. Higashino, M. & Stefan, H. G. Modeling the effect of rainfall intensity on soil-water nutrient exchange in flooded rice paddies and implications for nitrate fertilizer runoff to the Oita River in Japan. *Water Resour. Res.* **50**, 8611–8624 (2014).
43. Yoon, D. K. et al. Transgenic rice overproducing Rubisco exhibits increased yields with improved nitrogen-use efficiency in an experimental paddy field. *Nat. Food* **1**, 134–139 (2020).
44. Gravois, K. A. & Helms, R. S. Effect of uneven emergence on rice yield, milling yield, and yield components. *Aust. J. Exp. Agr.* **34**, 949–952 (1994).
45. Wang, S. A. et al. Reduced sediment transport in the Yellow River due to anthropogenic changes. *Nat. Geosci.* **9**, 38–41 (2016).
46. Ishibashi, M. & Terashima, I. Effects of continuous leaf wetness on photosynthesis—adverse aspects of rainfall. *Plant Cell Environ.* **18**, 431–438 (1995).
47. Bollen, K. A. Total, direct, and indirect effects in structural equation models. *Sociol. Methodol.* **17**, 37–69 (1987).
48. Wang, X. H. et al. Management outweighs climate change on affecting length of rice growing period for early rice and single rice in China during 1991–2012. *Agric. For. Meteorol.* **233**, 1–11 (2017).
49. Müller, C. et al. Global gridded crop model evaluation: benchmarking, skills, deficiencies and implications. *Geosci. Model Dev.* **10**, 1403–1422 (2017).
50. Wu, X. et al. ORCHIDEE-CROP (v0), a new process-based agro-land surface model: model description and evaluation over Europe. *Geosci. Model Dev.* **9**, 857–873 (2016).
51. Kobayasi, K., Matsui, T., Yoshimoto, M. & Hasegawa, T. Effects of temperature, solar radiation, and vapor-pressure deficit on flower opening time in rice. *Plant Prod. Sci.* **13**, 21–28 (2010).
52. Julia, C. & Dingkuhn, M. Variation in time of day of anthesis in rice in different climatic environments. *Eur. J. Agron.* **43**, 166–174 (2012).
53. Hempel, S., Frieler, K., Warszawski, L., Schewe, J. & Piontek, F. A trend-preserving bias correction—the ISI-MIP approach. *Earth Syst. Dyn.* **4**, 219–236 (2013).

Acknowledgements

This study was supported by the National Natural Science Foundation of China (42225102 and 41977082, F.Z.; 42007079, J.F.; 42171096, X.W.; 41530528, S.L.P). We acknowledge K. Liu, J. Wang and L. Shu from Jingzhou Agrometeorological Experimental Station, S. Wang, W. Adalibieke, Y. Bo, C. Wu, W. Jiang, M. Yuan, H. Cai and C. Wang from Peking University, X. Huang, L. Chen and D. Zhuang from Central China Normal University and C. Li from South China Sea Institute of Oceanography, Chinese Academic of Science for supporting field experiments and laboratory analyses. We acknowledge the CMA for nationwide observations of rice yield, phenology, hourly precipitation and extreme climate events, and the NASA for GPM IMERGv6 data.

Author contributions

F.Z. designed the study. Y.J., J.F. and X.W. performed all computational analyses. F.Z., X.W., J.F. and Y.J. drafted the paper. L.L. provided high-resolution climate projection using the IPSL model. All co-authors reviewed and commented on the paper.

Competing interests

The authors declare no competing interests.

Additional information

Supplementary information The online version contains supplementary material available at https://doi.org/10.1038/s43016-023-00753-6.

Correspondence and requests for materials should be addressed to Feng Zhou.

Peer review information *Nature Food* thanks David Makowski, Yan Li and the other, anonymous, reviewer(s) for their contribution to the peer review of this work.

nature portfolio

Corresponding author(s): Feng Zhou

Last updated by author(s): Apr 5, 2023

Reporting Summary

Nature Portfolio wishes to improve the reproducibility of the work that we publish. This form provides structure for consistency and transparency in reporting. For further information on Nature Portfolio policies, see our Editorial Policies and the Editorial Policy Checklist.

Statistics

For all statistical analyses, confirm that the following items are present in the figure legend, table legend, main text, or Methods section.

n/a	Confirmed
☐	☒ The exact sample size (*n*) for each experimental group/condition, given as a discrete number and unit of measurement
☐	☒ A statement on whether measurements were taken from distinct samples or whether the same sample was measured repeatedly
☐	☒ The statistical test(s) used AND whether they are one- or two-sided *Only common tests should be described solely by name; describe more complex techniques in the Methods section.*
☐	☒ A description of all covariates tested
☐	☒ A description of any assumptions or corrections, such as tests of normality and adjustment for multiple comparisons
☐	☒ A full description of the statistical parameters including central tendency (e.g. means) or other basic estimates (e.g. regression coefficient) AND variation (e.g. standard deviation) or associated estimates of uncertainty (e.g. confidence intervals)
☐	☒ For null hypothesis testing, the test statistic (e.g. *F*, *t*, *r*) with confidence intervals, effect sizes, degrees of freedom and *P* value noted *Give P values as exact values whenever suitable.*
☒	☐ For Bayesian analysis, information on the choice of priors and Markov chain Monte Carlo settings
☒	☐ For hierarchical and complex designs, identification of the appropriate level for tests and full reporting of outcomes
☐	☒ Estimates of effect sizes (e.g. Cohen's *d*, Pearson's *r*), indicating how they were calculated

Our web collection on statistics for biologists contains articles on many of the points above.

Software and code

Policy information about availability of computer code

Data collection	No software was used.
Data analysis	Our analyses were performed using R verson 4.1.2 (bootstrap t test was performed using R package MKinfer v.0.5 and structural equation modelling (SEM) implemented in the R package lavaan v.0.6-7) and MATLAB R2020a (MATLAB and Statistics Toolbox Release R2020a, The MathWorks), with the codes available from https://www.doi.org/10.6084/m9.figshare.19801765. Source codes for process-based model are available from http://forge.ipsl.jussieu.fr/orchidee, under the French Free Software license, compatible with the GNU GPL (http://cecill.info/licences.en.html). Installation guide for ORCHIDEE can be found at http://forge.ipsl.jussieu.fr/orchidee/wiki/Documentation/UserGuide/InstallingORCHIDEEBasic. The detail of use guide can be found at http://forge.ipsl.jussieu.fr/orchidee/wiki/Documentation/UserGuide.

For manuscripts utilizing custom algorithms or software that are central to the research but not yet described in published literature, software must be made available to editors and reviewers. We strongly encourage code deposition in a community repository (e.g. GitHub). See the Nature Portfolio guidelines for submitting code & software for further information.

Data

Policy information about availability of data

All manuscripts must include a data availability statement. This statement should provide the following information, where applicable:

- Accession codes, unique identifiers, or web links for publicly available datasets
- A description of any restrictions on data availability
- For clinical datasets or third party data, please ensure that the statement adheres to our policy

The data from the national agrometeorological observation network and the rainfall manipulative experiments are available in Supplementary Data 1. The climate data, records of extreme climate events, rice yield and phenology at the site scale from the China Meteorological Administration (CMA) are available at https://data.cma.cn/en. Model input data for historical simulations and future projections are available from public data depositories listed in Supplementary Table 5. The global precipitation measurement (GPM) IMERGv6 are available at https://disc.gsfc.nasa.gov/datasets/GPM_3IMERGHH_06/summary. Model output data for historical simulations and future projections are available in Supplementary Data 2. Source data are provided with this paper.

Human research participants

Policy information about studies involving human research participants and Sex and Gender in Research.

Reporting on sex and gender	We have no human study participants.
Population characteristics	We have no human study participants.
Recruitment	We have no human study participants.
Ethics oversight	We have no human study participants.

Note that full information on the approval of the study protocol must also be provided in the manuscript.

Field-specific reporting

Please select the one below that is the best fit for your research. If you are not sure, read the appropriate sections before making your selection.

☐ Life sciences ☐ Behavioural & social sciences ☒ Ecological, evolutionary & environmental sciences

For a reference copy of the document with all sections, see nature.com/documents/nr-reporting-summary-flat.pdf

Ecological, evolutionary & environmental sciences study design

All studies must disclose on these points even when the disclosure is negative.

Study description	We used long-term nationwide observations and multi-level rainfall manipulative experiments to explore the magnitude and mechanisms of extreme rainfall impacts on rice yield in China. We further improved a process-based crop model by explicitly accounting for the relevant mechanisms to hindcast and project the yield responses to extreme rainfall across China.
Research sample	Field observations of rice yield and extreme climate events were obtained from the national agrometeorological observation network. Global gridded hourly rainfall were accessed from GPM dataset. National gridded crop yields were simulated by a process model. We conducted rainfall manipulative experiments involving three rice growing seasons.
Sampling strategy	We used all available samples.
Data collection	The authors conducted rainfall manipulative experiments and performed crop model simulations. Field observations of rice yield, phenology, and extreme climate events can be accessed in http://data.cma.cn/. For historical simulations, climate forcing published by Sitch et al. (2015) were performed by Dr. Sitch, atmospheric CO2 concentration can be downloaded from https://gml.noaa.gov/ccgg/trends/, half-hourly rainfall can be downloaded from https://disc.gsfc.nasa.gov/datasets/GPM_3IMERGHH_06/summary, transplanting date were interpolated from site-level observations that were downloaded from http://data.cma.cn/, N application rate and rice sowing area published by Zhan et al. 2021 were performed by Dr. Zhan. For future projections, climate forcing, extreme rainfall intensity and event amount published by Yang et al. (2016) were performed by Dr. Yang, atmospheric CO2 concentration (RCP4.5, RCP8.5) published by Moss et al. (2010) were performed by Pro. Dr. Moss.
Timing and spatial scale	Field observations of rice yield and extreme climate events in China were analyzed over the period 1999-2012. The rainfall manipulative experiment was conducted in 2018, 2019 and 2021. Rice yield in China was simulated during 2001-2016 and 2085-2100.
Data exclusions	No data was excluded.

Reproducibility	Our study is an integrated study mainly based on manipulative experiments, field observations, and model simulations. Our results can be reproduced when following the described methods and data.
Randomization	This is not relevant to our study.
Blinding	This is not relevant to our study.

Did the study involve field work? ☒ Yes ☐ No

Field work, collection and transport

Field conditions	The rainfall manipulative experiment was conducted from 2018 to 2019, spanning two rice growing seasons. We manipulated rainfall levels by running the artificial rainfall manipulation system (NLJY-10, Nanlin Electronics, China) for one hour on two replicates for each treatment, with the rainfall amount of 60, 120, 180, and 240 mm. To isolate the mechanism driving the causal relationship between extreme rainfall and FG, we ran the first supplementary experiment during the reproductive phase in July 2021. To confirm the causal effect of extreme rainfall on EP, we ran the second supplementary experiment during vegetative phase in June 2021.
Location	It is at the Jingzhou Agrometeorological Experimental Station in Hubei province, China (30°21′N, 112°09′E).
Access & import/export	We have not access habitats.
Disturbance	Each plot was completely isolated by plastic-covering levees and impervious plates at a 0.5-meter distance in between to avoid mutual interference. Height of rainfall simulators was designed according to the height of rice plants to minimize disturbance when moving. Sample collections were conducted carefully by one people each time to reduce the contacting with other plants.

Reporting for specific materials, systems and methods

We require information from authors about some types of materials, experimental systems and methods used in many studies. Here, indicate whether each material, system or method listed is relevant to your study. If you are not sure if a list item applies to your research, read the appropriate section before selecting a response.

Materials & experimental systems

n/a	Involved in the study
☒	☐ Antibodies
☒	☐ Eukaryotic cell lines
☒	☐ Palaeontology and archaeology
☒	☐ Animals and other organisms
☒	☐ Clinical data
☒	☐ Dual use research of concern

Methods

n/a	Involved in the study
☒	☐ ChIP-seq
☒	☐ Flow cytometry
☒	☐ MRI-based neuroimaging